Optical selection rules and scattering processes in rocksalt wide band gap ZnO

H. W. Kunert*,1, M. Govender1,2, A. G. J. Machatine1, B. W. Mwakikunga2, and P. Niyongabo1

[1] Department of Physics, University of Pretoria, Pretoria 0002, South Africa
[2] DST/CSIR National Centre for Nano-Structured Materials, CSIR, P. O. Box 395, Pretoria, 0001, South Africa

At sufficiently high pressures, wurtzite structure zinc oxide (W-ZnO) can be transformed to the cubic rocksalt (R-ZnO) structure. The R-ZnO exhibits semiconductor behavior with an indirect wide band gap of $E_g = 5.5$ eV. The maximum valence band is found far away from the center of the Brillouin zone (BZ) at high symmetry point L and line Σ, depending on the pressure. The unusual electronic band structure (EBS) of the R-ZnO leads to several direct and indirect optical transitions which find applications in ultraviolet optoelectronic devices. We have investigated radiative and non-radiative symmetry restricted selection rules, as well as inter- and intra-valley scattering processes.

1 Introduction The R-ZnO structure (R-O_h^5, $Fm3n$ space group) has recently attracted much attention due to an unconventional EBS that can be used in mechanical and optoelectronic applications [1–4]. Jaffe et al. [5] calculated the EBS of R-ZnO by the all-electron local-orbits Hartree–Fock method along some major symmetry lines and points, shown in Fig. 1a. Some symmetry assignments are contrary to that commonly accepted, for example, the band structure of R-ZnO in [5], which is presented in Fig. 1b, where one of the VB maximum has W_1 symmetry instead of W_5 symmetry, and the K point seems to be incorrectly assigned. Reference to group theoretical assignments has not yet been provided.

Segura et al. [6] reported on pressure dependence of the optical absorption edge in R-ZnO up to 20 GPa measured at room temperature. The low-energy tail of the absorption has been assigned to an indirect transition. Figure 2 shows the EBS of R-ZnO along some high symmetry directions of the BZ at several pressures. The minimum of the lowest conduction band (CB) remains at the center of the BZ (point Γ), while the highest maximum of the valence band (VB) occurs on the Σ-line and at the L point. No group theoretical assignments of electron and hole states have been discussed, and therefore no optical selection rules (OPSRs) have been considered. Based on pressure absorption dependence, the optical absorption leads to indirect transitions: L–Γ, Σ–Γ as well as direct transitions at X, L, and high symmetry points have been assigned by us using a group theoretical approach. In this paper, we provide rigidly calculated OPSRs for all transitions, as well as selection rules for possible inter- and intra-valley scattering processes.

In Section 2 of this paper, we discuss assignments of electrons and holes in CBs and VBs needed for determination of OPSRs. In Section 3, we deal with the general quantum mechanical rules needed for matrix element transitions. In Section 4, we discuss the wave vector selections rules (WVSRs) which follow from the momentum conservation principle. The direct radiative transition selection rules (DrTrSRs) and the symmetry of excitons are discussed in Section 5. The indirect transitions (InDrTrs) involving vibrational modes are considered in Section 6. In the last section we discuss our results and predictions regarding the splitting of L excitons.

2 Symmetry assignments of electron and hole states in the conduction and valence bands in R-ZnO The states of electrons and holes in a crystal are characterized by the wave vector k and the irreducible representations (irrps) of a space group $G(k)$. When the spin of a particle or quai-particle is disregarded, the states are classified according to the so-called single-valued irrps (SVirrps). The inclusion of spin leads to double-valued irrps (DVirrps) known as spinors. The EBS can be determined by several experimental techniques such as absorption, Raman, photoluminescence and reflectivity spectroscopies.
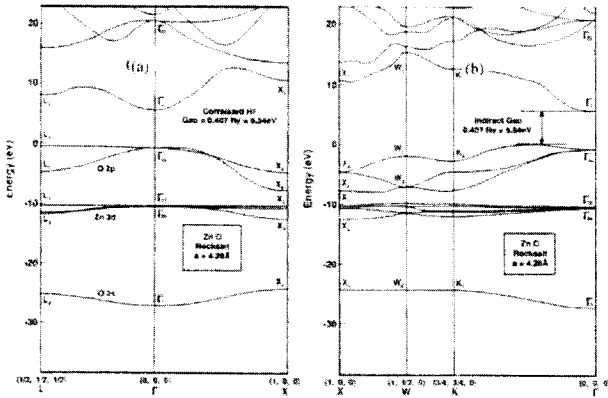
Figure 1 (a) Correlation-corrected Hartree–Fock band structure of ZnO in the rocksalt structure and (b) correlation-corrected Hartree–Fock band structure of ZnO in the rocksalt structure for some additional directions in reciprocal space. Diagrams adopted from Ref. [5].

Segura et al. [6] did not take into account SRs for their high symmetry points, so based on group theoretical techniques, we have determined the major high symmetry line and points of the respective BZ according to the irrps of O_h^5 space group using Cracknell, Davies, Miller and Love Tables (CDML) labeling [7]. In Table 1, we list the respective states of electron and holes in terms of CDML labeling of irrps in CBs and VBs. In Table 2, we show a correspondence of irrps labeling between Bouckaert, Smoluchowski and Wigner (BSW) [8] Jaffet and Koster (JK) [9], and CDML tables.
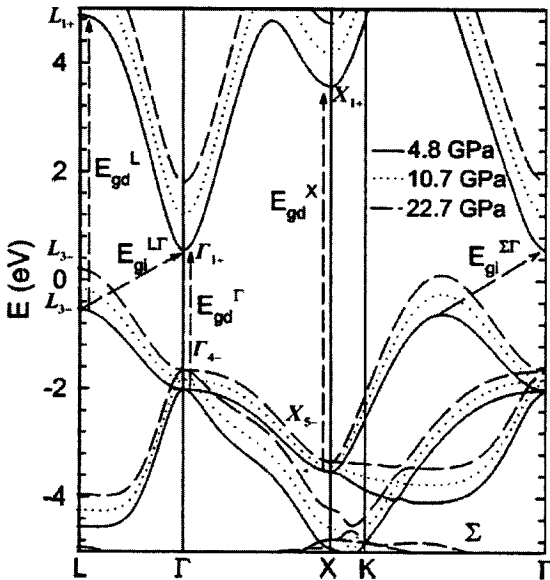
Figure 2 Electronic band structure of rocksalt ZnO along high-symmetry directions of the BZ at several pressures, as calculated through *ab initio* DFT-LDA pseudopotential method. Diagram adopted from Ref. [6].

Table 1 Symmetry assignment of high symmetry points in cubic R-ZnO.[a]

single-valued representations–spin excluded			
conduction bands	L_{1+}	Γ_{1+} (lowest)	X_{1+}
valence bands	L_{3-} (highest)	Γ_{4-}	X_{5-}
double-valued representations–spin included			
conduction bands	L_{6+}	Γ_{6+}	X_{6+}
valence bands[b]	L_{4-}, L_{5-}, L_{6-}	Γ_{8-}, Γ_{6-}	X_{7-}, X_{6-}

[a]The assignment is in terms of CDML irreducible representations. The double-valued representations have been obtained by multiplication of the single-valued representations by two-dimensional representations (spinor representation $D_{(1/2)}$ CDML [7], p. 9);
[b]Due to possible spin–orbit interactions, the valence band L_{3-} (two-dimensional, small representation) $\times D_{(1/2)}$ splits onto L_{4-} (one-dimensional), L_{5-} (one-dimensional) and L_{6-} (two-dimensional) representations. Similar effects happen for Γ_{6+} and X_{6+} representations.

Table 2 Labels of irreducible representations for the point Γ for O_h^5–$Fm3n$ space group of R-ZnO.[a]

JK [8]	BSW [9]	CDML [7]
Γ_{1+}	Γ_1	Γ_{1+}
Γ_{2+}	Γ_2	Γ_{2+}
Γ_{3+}	Γ_{12}	Γ_{3+}
Γ_{4+}	$\Gamma_{15'}$	Γ_{4+}
Γ_{5+}	$\Gamma_{25'}$	Γ_{5+}
Γ_{1-}	$\Gamma_{1'}$	Γ_{1-}
Γ_{2-}	$\Gamma_{2'}$	Γ_{2-}
Γ_{3-}	Γ_{12+}	Γ_{3-}
Γ_{4-}	Γ_{15+}	Γ_{4-}
Γ_{5-}	Γ_{25}	Γ_{5-}

[a]For more details, see Ref. [10], p. 533.

3 Selection rules We first recall the basic theorems on SRs [9]. The study of an absorption or scattering cross section for a process involving the absorption or scattering of particles or quasi-particles with wave vector k in a crystal involves the calculation of transition probabilities, which in turn involves the calculation of quantum mechanical matrix elements. The matrix elements of a perturbation f between an initial and final state are of the form $V_{pq}^{\mu\nu} = \left\langle \psi_q^\mu |f| \psi_p^\nu \right\rangle$, where ψ_q^μ and ψ_p^ν are the wave functions (with respective basis functions for irrps D^μ and D^ν) of the particle or quai-particles involved in the absorption or scattering processes.

Acting by symmetry operators of a given space group on the matrix elements (wave functions and perturbation operator f, we obtain the Kronecker product (KP) between three irrps $D^\mu \times D^f \times D^\nu$. When the KP contains the unit representation, normally denoted as Γ_1, Γ_{1+} or A_1, the transition between states due to perturbation f is allowed, otherwise it is forbidden. The square of any irrps always contains the identity representation. Therefore, it suffices to consider only single KPs between two irrps and check whether the third representation is in the decomposition. All

possible KPs for 230 space groups have been tabulated in CDML.

4 Momentum conservation principles: Wave vector selection rules

An electron in a state k can be scattered into another state k' due to an interaction with a phonon at the k'' state. The momentum conservation $k + k' = k''$ determines the WVSRs. The WVSRs originate from appropriate combinations of arms of stars $*k$, $*k'$ and $*k''$[11]. For face-centered cubic crystals with tetragonal and cubic symmetries (T_d^2, O_h^5, and others), the WVSRs have been tabulated in Table 2. In R-ZnO, there are three pronounced valleys at Γ, L, and X points. The star of the L valley is $*k(L)$: kL, $2kL$, $3kL$, and $4kL$, and the star of the X valley is kX, $5kX$, and $9kX$. At the Γ point, we have only one wave vector $k = 0$. The numbers 1, 2, 3, 4, 5, and 9 denote the symmetry operators of O_h^5 group [7]. The first minima at each of these points are characterized by the first wave vectors $k = 0$, kL, and kX in the fundamental domain of the BZ. It means that we deal with four non-equivalent L valleys, three X and one Γ valley. The inter- and intra-valley scattering processes are subjected to WVSRs and are discussed in Section 6.

5 Direct radiative transition selection rules in R-ZnO

5.1 Point Γ

At point Γ, the momentum of the electron and hole are very small (almost zero). The respective KP of a radiative transition from the minimum CB of Γ_{1+} symmetry (spin of electron and hole excluded) to the maximum of the VB of Γ_{4-} symmetry (Table 1) due to the laser beam with electric field $E = E_0 \exp(kr - \omega t)$, (E_x, E_y, E_z) which transforms like an ordinary vector x, y, z. Therefore, according to Γ_{4-} representation (VR) is of the form: $\{(\Gamma_{1+}) \times (\Gamma_{4-}) \times (\Gamma_{4-})\}$. The KP contains the identity representation and therefore the direct transitions at Γ are in accordance with absorption measurements [6].

5.2 Points L and X

The appropriate WVSR for direct transitions between the minimum of the L's CB of L_{1+} symmetry and the maximum of VB of L_{3-} symmetry is $kL + kL = kG$ in channel Γ and $kL + 3kL = kX$, $kL + 2kL = 5kX$, and $kL + 4kL = 9kX$ in the X channel. The SR is $\{L_{1+}(\text{CB}) \times L_{3-}(\text{VB}) \times \Gamma_{4-}\} = (\Gamma_{3-} + \Gamma_{4-} + \Gamma_{5-}) \times (\Gamma_{4-})$ in the Γ channel and $(X_{1-} + X_{2-} + X_{3-} + X_{4-} + 2X_{5-})$ in the X channel. Clearly the KP contains the identity representation Γ_{1+}. Consequently, the direct transitions at the L point are allowed in accordance with experimental data [6].

For point X, we have $kX + kX = kG$ in the Γ channel and $kX + 5kX = 9kX$ for the X channel, respectively. The respective KP is of the form $\{(X_{1+}) \times (X_{5-}) \times (\Gamma_{4-})\} = (\Gamma_{1-} + \Gamma_{5-}) \times \Gamma_{4-}$, in the Γ channel and for the X channel $(X_{3-} + X_{4-}X_{5-}) \times \Gamma_{4-}$. Again the transitions are allowed, as confirmed by Segura et al. [6].

5.3 Σ line

Inspecting Fig. 2 [6], we note that the transition from Σ-VB to Σ-CB needs a very high energy laser beam. Therefore, we will not consider this transition. Nevertheless, the indirect transition Σ–Γ is of interest and we will discuss them here.

5.4 Spin inclusion and excitons in R-ZnO

The EBS have been studied by several authors [5, 6]. They have not taken spin of electrons and holes into consideration. The hexagonal W-ZnO, from which the R-ZnO has been made, experiences strong magnetic properties evidenced by pronounced spin–orbit (S–O) interaction values. The strong magnetic properties and crystalline field split the VB into three sub-bands which contribute to the three A, B, and C excitons, and are seen by reflectance, photoluminescence and absorption techniques.

We believe that R-ZnO will also exhibit some magnetic properties that require an inclusion of spin. To our best knowledge, there are no magnetic experimental data on R-ZnO available. Nevertheless, we include the spin to our considerations in OPSRs in an attempt to predict some new features. When spin is included, the states of particles or quasi-particles are classified according to DVirrps. We have calculated the double-valued representation $D_{(1/2)}$ [11], reduced to the symmetry operations of O_h^5 group for points Γ, L, and X using Eq. (9.65) and Table 3.1 in Ref. [7]. With the help of the $D_{(1/2)}$ representation, we were able to determine the spinor representations for the R-ZnO at high symmetry points. The inclusion of electron spin in CBs results in the classification of states in terms of the spinor representations: $\Gamma_{6+} = \Gamma_{1+} \times D_{(1/2)}$, $L_{6+} = L_{1+} \times D_{(1/2)}$ and $X_{6+} = X_{1+} \times D_{(1/2)}$. All the representations are now doubly degenerate.

The holes in the VBs after an inclusion of spin are classified according to the following DVirrps: Γ_{8-} and Γ_{6-} contained in $\Gamma_{4-} \times D_{(1/2)}$; L_{4-}, L_{5-}, and L_{6-} contained in the KP: $L_{3-} \times D_{(1/2)}$ and X_{6+} in $X_{1+} \times D_{(1/2)} = X_{6+}$. It means that the state L_{3-} of the holes at the highest VB maximum at L point splits into three VBs (when spin is included) of L_{4-}, L_{5-}, and L_{6-} symmetries each of them twofold degenerated. Similarly, holes at the Γ split onto fourfold degenerate (Γ_{8-}) heavy and two-fold degenerate (Γ_{6-}) light holes like states of holes in Si and Ge and GaAs.

Consequently, several direct and indirect excitons are expected to be observed experimentally. For direct L excitons we have three types of them as: $L_{6+} \times L_{4-}$ (let's call them L_1 excitons), $L_{6+} \times L_{5-}$ (L_2 excitons) and $L_{6+} \times L_{6+}$ (L_3 excitons). This is in analogy to W-ZnO's A, B, and C, Γ excitons [11]. We believe that the magneto-photoluminescence, reflectance and absorption will confirm our predictions. The R-ZnO structure (R-O_h^5, $Fm3n$ space group) has recently attracted much attention due to an unconventional EBS that can be used in mechanical and optoelectronic applications

6 Indirect electronic transitions and inter and intra-valley scattering processes in R-ZnO

6.1 Electronic indirect transitions in R-ZnO

The vertical direct radiative transitions preserve the k vector and

InDrTrs involve participation of phonons. We must distinguish between the two kinds of InDrTrs; those with inclusion of electron and hole spin dependent on the magnitude of S–O interactions and those without. When S–O, spin–spin (S–S), or spin–lattice (S–L) interactions are neglible, we deal with SVirrps which are the classification of electron and hole states. In such cases of the InDrTrs in R-ZnO, an electron in the CB can drop radiatively from L_{1+} to L_{3-} and then be scattered in the VB by a phonon from L_{3-} to the Γ_{4-} VB. In the process, the radiative transition from L_{1+} to L_{3-} is allowed as discussed in Section 5. The scattering processes in the VB requires KP: $L_{4-} \times \Gamma_{4-} = L_{1+} + L_{2+} + 2L_{3+}$. The decomposition of the KP clearly indicates the symmetry allowed phonons: L_{1+} (no phonon), L_{2+} (longitudinal acoustic LA phonon), and L_{3+} (transverse acoustic TA phonon). In the second scattering process, an electron can be scattered from the L_{1+} to the Γ_{1+} CB, described by KP $L_{1+} \times \Gamma_{1+} = L_{1+}$ (longitudinal optical LO phonon) and then drop radiatively from Γ_{1+} to Γ_{4-}, which is allowed.

6.2 Inter- and intra-valley scattering processes in R-ZnO

Regarding the theory of inter-valley scattering (InterVSc) and intra-valley scattering (IntraVSc) processes, we refer to the work by Lax–Hopfield (LH), and Birman–Lax–Loudon (BLL) [12, 13]. More about the IntraVSc by acoustic and optical phonons and InterVSc in GaAs, Si, and Ge [14]. Recently, Kunert et al. [15] considered the scattering processes in hexagonal W-ZnO.

In this section, we determine the allowed symmetries of vibrational modes of an electron scattered from one valley to another. There are three different scattering processes involved. In R-ZnO [5, 6], the electronic bands resolve valleys at Γ, (Γ_{1+}), $K(K_1)$, $V(V_1)$, and possibly $L(L_{1+})$ points. Point X consists of three non-equivalent valleys with electrons at kX, $5kX$, and $9kX$ states, while at point L we deal with four non-equivalent valleys with electrons of kL, $2kL$, $3kL$, and $4kL$ momentum. The IntraVSc means scattering of electrons within three valleys at X point or within four valleys at the L point, while InterVSc refers to scattering processes between three X valleys and four L valleys. Theses scattering processes involve KPs between SVirrps (no-spin). Here we consider the following KPs for InterVSc: $\Gamma \times X$, $\Gamma \times L$, $\Gamma \times V$ and for IntraVSc: $\Gamma \times X$, $X \times X$, and $L \times L$.

For InterVSc we have: $\Gamma_{1+} \times X_{1+} = X_{1+}$ (LO and LA phonons dependent on masses of ions), $\Gamma_{1+} \times L_{1+} = L_{1+}$ (LO and LA phonons), and $\Gamma_{1+} \times V_1 = V_1$ (unknown). Our predictions of phonon symmetries participating in scattering processes is based on group theoretical connectivity relations. To the best of our knowledge, there are no experimental data on phonon dispersion curves and phonon density of states in R-ZnO.

In an IntraVSc process, which means scattering within or between valleys belonging to the same star, two kinds of phonons are involved, phonons with large momentum like hkL, hkW, or hkX and with very low momentum $hk = 0$. The IntraVSc requires a special symmetric KP [11], and for R-ZnO, take the form $[\Gamma_{1+} \times \Gamma_{1+}]_2 = \Gamma_{1+}$, $[X_{1+} \times X_{1+}]_2 = \Gamma_{1+} + \Gamma_{3+}$, and $[L_{1+} \times L_{1+}]_2 = \Gamma_{1+} + \Gamma_{5+}$ for low momentum of Γ phonons and $[X_{1+} \times X_{1+}]_2 = X_{1+}$ and $[L_{1+} \times L_{1+}]_2 = X_{1+} + X_{4+}$ for large phonon momentum. Consequently, phonons involved in IntraVSc in R-ZnO are of symmetries: Γ_{1+} (TA and LA), Γ_{3+}, Γ_{5+} (TO and LO), and X_{4+} (TO).

7 Discussion

We have derived optical selection rules based on the assignments of electronic bands listed in Table 1. We believe that electron states in CBs with no spin (Γ_{1+}, L_{1+}, and X_{1+}) and with spin (Γ_{6+}, L_{6+}, and X_{6+}) are properly assigned. Experimentally, it has been shown that the VB maxima in R-ZnO are at L point and Σ line, but not at the center of the BZ (Γ point). In many compounds, the highest VB maximum is at the Γ point and holes states (p_x, p_y, p_z) which transform as the VR. Since the center of the BZ is of the highest symmetry, we assigned it as Γ_{4-} = VR (no spin). The highest VB maximum has been assigned by L_{3-} two-dimensional representations according to which holes (p_x, p_y) supposed to transform. Our OPSRs are based mainly on theoretical derivations and are in agreement with absorption data. There is a lack of experimental data on R-ZnO, such as Raman, photoluminescence, and reflectance spectra. There is also no phonon dispersion relation and density of phonon states measured by X-ray and neutron scattering techniques. The forthcoming experimental work will verify our selection rules.

8 Conclusions

An attempt has been made on assignments of the EBS of R-ZnO. Some optical selection rules related to direct and indirect transitions were discussed. Splitting of the maximum VB at point L due to possible S–O interaction onto three sub-bands of L_{4-}, L_{5-}, and L_{6-} symmetries, may result in the three observed exciton bands. We hope that magneto-photoluminescence and reflectivity will prove our predictions. It is well known that in the W-ZnO at point Γ, three excitons A, B, and C contribute to the optoelectronic devices application. It would mean that by pressure, one can "shift" the A, B, and C parabolic excitons in W-ZnO to the $L_1(L_{4-})$, $L_2(L_{5-})$, $L_3(L_{6-})$, and non-parabolic ones in R-ZnO.

References

[1] C. W. Litton, D. C. Reynolds, and T. C. Collins, Zinc Oxide Materials for Electronic and Optoelectronic Device Applications, Technology and Engineering (John Wiley & Sons, New York, 2011).

[2] K. Li, C. Kang, and D. Xue, Mater. Res. Bull. 47, 2902–2905 (2012).

[3] H. Y. Wu, X. L. Cheng, C. H. Hu, and P. Zhou, Physica B 405, 606–612 (2010).

[4] M. J. S. Spencer, Progr. Mater. Sci. 57, 437–486 (2012).

[5] J. E. Jaffe, R. Pandey, and A. B. Kunz, Phys. Rev. 43, 14030 (1991).

[6] A. Segura, J. A. Sans, F. J. Manjon, A. Munoz, and H. Cabrera, Appl. Phys. Lett. 83, 278 (2003).

[7] A. P. Cracknell, B. L. Davies, S. C. Miller, and W. F. Love, Kronecker Product Tables, Vols. 1–4 (IFI/Plenum, New York, Washington, London, 1979).

[8] L. P. Bouckaert, R. Smoluchowski, and E. Wigner, Phys. Rev. **50**, 266–280 (1936).

[9] M. Hamermesh, Group Theory and Its Application to Physical Problems (Addison-Wesley Publ. Co., Inc., Reading, Massachusetts, London, 1962).

[10] H. W. Kunert, J. Popenda, and M. Suffczynski, J. Physique **39**, 526 (1978).

[11] H. W. Kunert, Cryst. Eng. **4**, 233–240 (2001).

[12] M. Lax and J. J. Hopfield, Phys. Rev. **124**, 115 (1961).

[13] J. L. Birman, M. Lax, and R. Loudon, Phys. Rev. **145**, 620 (1966).

[14] Y. Yu and M. Cardona, Fundamentals of Semiconductors, Physical and Material Properties (Springer-Verlag, Berlin, Heidelberg, New York, 1966).

[15] H. W. Kunert, M. R. Wagner, A. G. J. Machatine, P. Niyongabo, J. B. Malherbe, A. Hoffmann, J. Barnas, and W. Florek, Phys. Status Solidi B **247**(7), 1802–1806 (2010).